



The toxic effect of CuO of different dispersion degrees on the structure and ultrastructure of spring barley cells (*Hordeum sativum distichum*)

Aleksei G. Fedorenko · Tatiana M. Minkina · Natalia P. Chernikova · Grigoriy M. Fedorenko · Saglara S. Mandzhieva · Vishnu D. Rajput · Marina V. Burachevskaya · Victor A. Chaplygin · Tatiana V. Bauer · Svetlana N. Sushkova · Aleksandr V. Soldatov

Received: 29 September 2019 / Accepted: 21 January 2020
© Springer Nature B.V. 2020

Abstract Nowadays, nanotechnology is one of the most dynamically developing and most promising technologies. However, the safety issues of using metal nanoparticles, their environmental impact on soil and plants are poorly understood. These studies are especially important in terms of copper-based nanomaterials because they are widely used in agriculture. Concerning that, it is important to study the mechanism behind the mode of CuO nanoparticles action at the ultrastructural intracellular level. It is established that the contamination with CuO has had a negative influence on the development of spring barley. A greater toxic effect has been exerted by the introduction of CuO nanoparticles as compared to the macrodispersed form. A comparative analysis of the toxic effects of copper oxides and nano-oxides on plants has shown changes in the tissue and intracellular levels in the barley roots. However, qualitative

changes in plant leaves have not practically been observed. In general, conclusions can be made that copper oxide in nano-dispersed form penetrates better from the soil into the plant and can accumulate in large quantities in it.

Keywords Soil · Plants · Cu oxide · Nanoparticles · Spring barley · Cell · Toxic effect · TEM

Introduction

Today nanotechnology is one of the most dynamically developing and most promising technologies. Nanoparticles (1–100 nm in size) can linger for a long time in the environment. They can also be absorbed and moved between organisms of different trophic levels undergoing biodegradation and bioaccumulation along the food chain (Ma et al. 2010; Morgalev et al. 2010; Anjum et al. 2013; Keller et al. 2013; Kulizhsky et al. 2013; Conway et al. 2014; Rajput et al. 2019, 2020).

Nanoparticles size directly affects their behavior, transport and fate in the environment. Nanoparticles that are of small diameter can be highly mobile, which could enhance their bioavailability compared to larger particles (Darlington et al. 2009; Guzman et al. 2006; Lecoanet et al. 2004; Phenrat et al. 2009). In contrast to a large number of studies focusing on their toxic effect of heavy metals in macrodispersed form (more

A. G. Fedorenko · T. M. Minkina (✉) · N. P. Chernikova · G. M. Fedorenko · S. S. Mandzhieva · V. D. Rajput · M. V. Burachevskaya · V. A. Chaplygin · T. V. Bauer · S. N. Sushkova · A. V. Soldatov
Southern Federal University, 105 Bolshaya Sadovaya Str., Rostov-on-Don, Russia 344006
e-mail: tminkina@mail.ru

A. G. Fedorenko · G. M. Fedorenko · T. V. Bauer
Federal Research Center the Southern Scientific Center of the Russian Academy of Sciences, Chehova St., Rostov-on-Don, Russia 344006

than 100 nm) on soil, plants and microbiota, there are not enough comprehensive studies on the toxicity of metal nanoparticles (Oberdörster et al. 2007; Kahru and Ivask 2013; Hu et al. 2014). The safety issues of using metal nanoparticles, their environmental impact are especially important in terms of copper-based nanomaterials, because they are widely used in the production of biocides in agriculture, for the wood protection and as antifouling agents (Navratilova et al. 2015; McVay et al. 2019). The accumulation of CuO nanoparticles in soil and groundwater can potentially lead to their accumulation in plant tissues. Copper oxides in the form of nanoparticles are not only toxic to plants, but also to human cells (Assadian et al. 2017). Cu^{2+} ions released from the surface of metal oxide nanoparticles are the main reason for their high toxicity to living organisms (Gabbay et al. 2006; Gunawan et al. 2011). Large amounts of Cu^{2+} can be released from copper oxide nanoparticles both in suspension and in the cell medium (Gunawan et al. 2011). Copper nanoparticles can catalyze the production of free radicals and the Fenton reaction damaging lipids, proteins and nucleic acids (Hänsch and Mendel 2009; Ivask et al. 2010; Festa and Thiele 2011; Hartwig 2013).

Recent studies indicated that the negative effects in toxicity of copper salts or ions compared to copper nanoparticulates were not fully caused by released Cu ions from the particles, but primarily induced nanoparticle specific (Griffitt et al. 2009; Gomes et al. 2011; Julich and Gäth 2014). The impact of CuO nanoparticles on agricultural plants caused changes in the structure of roots and leaves at the tissue and cellular levels negatively affecting plant growth and development, germination, photosynthesis, transpiration rate, crop yield and quality.

Shaw and Hossain (2013) reported significant inhibition in seed germination below 0.5 mM nano-CuO treatment. Study conducted by Zuverza-Mena et al. (2015) on CuO nanoparticles reduced more than 50% seed germination of cilantro (*Coriandrum sativum*). It is reported that the exposure to 100 and 500 mg L^{-1} copper nanoparticles reduced photosynthetic rate, plant biomass and transpiration rates of *Cucurbita pepo* in hydroponically grown (Musante and White 2012). In soil, 200 mg kg^{-1} CuO nanoparticles reduced leaf starch content, total sugar, reducing sugar and affected agronomical traits of *Origanum vulgare* (Du et al. 2018). Similar studies with *H.*

sativum indicated that the high concentration of CuO nanoparticles reduced root and shoot length, affected stomatal aperture and root morphology, reduced metaxylem number, affected chloroplast and mitochondrial ultrastructure (Rajput et al. 2018a, b).

The application of CuO nanoparticles deformed stomatal aperture of *Oryza sativa* and *Lactuca sativa* and severely affected net photosynthetic activities by affecting PS II reaction centers, and might cause a decrease in electron transport, thylakoid number per granum, photosynthetic rate, transpiration rate and stomata conductance (Costa and Sharma 2016; Xiong et al. 2017). These studies were carried out at the anatomical and histological levels (organs and tissues). They were limited only by morphological parameters and did not consider ultrastructural changes in plants. In this regard, it is important to study the mechanism behind the mode of action of CuO nanoparticles at the ultrastructural intracellular level.

Materials and methods

Soil preparation and plant growth

To study the toxic effect of Cu with different particle sizes on the structure of root cells and barley leaves, Haplic Chernozem was used in model experiment. Soil samples (layer 0–20 cm) were collected at the Specially Protected Natural Territory “Persianovskaya steppe” in Rostov Region (Russia). The experiment was carried out in plastic vessels with a closed drainage system, each of which was filled with 2 kg of soil. The experimental design included unpolluted soil (control) and experimental variants with soil contamination of CuO in macrodispersed and nano-dispersed forms (nano-CuO) at doses of 300 and 2000 mg/kg.

The dose of 300 mg/kg CuO nanoparticles in the soil corresponds to the level of soil pollution with Cu in Rostov region (Russia) (Minkina et al. 2017). A dose of 2000 mg/kg Cu is critical for crops (Dmitrakov and Dmitrakova 2006). Using such a dose of metal allows identifying the mechanisms of its transformation in the soil and the associated toxic effect on plants.

To saturate the soil, reference CuO compounds were used in a macrodispersed form (particle size

3–5 mm, analytical-grade reagent, CuO, divalent copper oxide, State Standards 16539-79) and in a nano-dispersed form (particle size—less than 30–50 nm, CAS-1317-38-0, Alfa Aesar, USA).

The seeds of two-row barley spring barley (*Hordeum sativum distichum*) of the Ratnik variety, which is one of the most significant and widely used food crops in the world (Arendt and Zannini 2013), were sown 8 months after copper oxide had been applied. It was shown this time is enough for the transformation of copper compounds in soil (Bauer et al. 2018). This species is used as a bioindicator to assess the effects of the content and accumulation of heavy metals. Vegetative growth of plants took place under natural light; the lowest field moisture capacity was maintained in the soil. The experiment was conducted three times.

Plant sampling and preparation for anatomical and ultrastructural observation

To study the toxicity of copper to morphometry of spring barley and cells ultrastructure, plants were selected at the booting stage. At this phase, barley is very sensitive to water deficiency, nutrients and other factors for life.

To conduct light-optical and electron microscopic studies, fragments were excised from the central part of the second or third leaf (2×2 mm) and the middle part of the root (2 mm). Root samples were collected from the root hair zone. Samples were fixed in a 2.5% solution of glutaraldehyde in phosphate buffer (pH 7.4) for 2 h in a vacuum at room temperature. After being washed twice with sucrose phosphate buffer, the samples were fixed with a 1% solution of OsO₄ for 2 h at room temperature. Then, the plant tissue was dehydrated in a graded series of ethanol of increasing concentrations (50%, 70%, 96%, respectively). Before being placed in 96% alcohol, the samples were kept in a 70% alcoholic uranyl acetate for 12 h in the cold (+ 4 °C). Then, they were washed off uranyl acetate and placed in absolute ethanol and acetone to continue dehydration three times for 15 min each time. Leaf cuttings were impregnated with resin in a series of solutions of Epon and acetone of increasing concentrations with a further immersion in Epon. The polymerization was carried out in a thermostat at a temperature of 37 °C (1 day), 60 °C (2 days). All stages of tissue preparation for morphological observation (contrasting, dehydration, encapsulation by

polymerization, preparation and staining of semi-thin sections for light-optical study) were performed using standard methods (Usatov et al. 2004, Fedorenko et al. 2018).

To perform light-optical observation, semi-thin sections with 0.5–1 µm thickness were additionally stained with methylene blue and examined using a LOMO light-optical microscope (Russia) at magnifications of $\times 100$ and $\times 400$. Ultrathin sections were obtained with Leica EM UC6 Ultramicrotome (Germany) and were additionally contrasted with lead citrate. The study was carried out using a transmission electron microscopy (TEM) (Tecnai G2, Phillips, Holland) in the Centre of Collective Usage “Modern Microscopy” of Southern Federal University. To X-ray spectral analysis (TEM–EDX) sample, slices were prepared with 150 nm thickness, fitted on a nickel mesh and not stained with lead citrate.

Elemental analysis of barley plant sections was performed by energy-dispersive X-ray spectroscopy (TEM–EDX) using FEI Tecnai G2 F20 transmission electron microscope with an EDAX (Apollo XLT model) at an accelerating voltage of 200 kV and a Fischione Instruments Model 3000 STEM detector in Microanalysis Shared Resource Center at Skolkovo Technology Park. To perform the measurements, an image area containing segments most saturated with electron-dense material was selected.

Morphometric analysis of light-optical images included the calculation of the area and the average number of cells per unit area of the leaf tissue, the average thickness of the leaf plate, the cut area of the root, the cut area of the central cylinder and the total cut area of the conducting tissues. Quantitative analysis of electron diffraction patterns took into account the average number of plastids per unit area of the leaf tissue, the average number of plastids per cell, as well as a visual analysis of the electron-dense sediment in the intercellular space and vacuoles. To measure cell fragments, Olympus Soft Imaging Solution iTEM automated microimage analysis system was used.

The mathematical processing of experimental data was carried out using MS Excel and Statistica 10 software. The reliability of the data was evaluated by Student's *t* test.

Results

The application of CuO in macrodispersed and (nano)dispersed forms influenced the growth and development of spring barley. Visual observations showed that at a dose of Cu 300 mg kg⁻¹ in the macrodispersed or (nano)dispersed forms, no noticeable changes in plant height were observed. At the same time, in variants with a higher dose of metal (2000 mg kg⁻¹), a significant decrease in plant height occurred. Soil pollution by copper not only affected the morphological parameters of barley, but also caused changes in the tissues and cells of plants.

Roots

Control

Light-optical studies have shown that the control samples of spring barley have the anatomical structure of the root typical of monocotyledonous plants (Tutayuk 1972). The outermost layer of the root is a single layer of *epidermis*. The epidermal cells are live, on the periphery, they are elongated and form root hairs (Fig. 1a). Cells of the cortex are under the epidermis layer. The innermost layer of the cortex forms the endoderm. Endoderm cells are located in 1–2 layers and are closely adherent to each other. Their outer walls are thin, and inner and radial (side) walls are significantly thickened. Among the cells of the endoderm, there are single cells with unthickened walls, rich in contents (passage cells).

The central cylinder that occupies about 20% of the total root section in the control sample consists of a pericycle and conducting tissues (Fig. 1a). Pericycle cells are larger, slightly elongated along the radius. Behind the pericycle, there is the parenchymal tissue with the conducting elements being immersed into. The vessels of xylem rays have narrower gaps toward the periphery and larger toward the center. Between the xylem rays in the upper part, there are sections of the phloem composed of sieve tubes with companion cells.

Morphometric analysis has shown that the average cortical cell size is 430 μm², the average number of cells per 1 mm² is 3773 and the ratio of conducting tissue area to the total section area is 0.17 (Table 1).

Electron microscopic analysis has shown that the control plant roots have normal ultrastructural characteristics in the cells, with intact cell walls, a large

central vacuole, granular reticulum (Fig. 2a), mitochondria (Fig. 2a insert) and the nucleus.

CuO contamination

The anatomical root structure of the barley samples grown in the soil contaminated with copper oxide has a number of significant differences compared to the control samples. The outermost layer of the root is a single layer of epidermis. The epidermal cells are live, and on the periphery, they are elongated and form root hairs (Fig. 1b, c). However, in contaminated samples, they are shorter and thicker than in the control, which reduces the surface area.

In the control samples, there is a rather large intercellular space between the parenchyma cells, and in the contaminated ones, there is very little intercellular space. Parenchyma cells are closely adjacent to each other. Therefore, with the same cell sizes in contaminated samples of cells, there is more per unit area.

Cells of the primary cortex are below the epidermis layer. Compared with the control, contaminated samples demonstrate a significant reduction of this layer that ranges from one to four layers of cells depending on the copper oxide dose. Endoderm cells are arranged in 1–2 layers and are closely adherent to each other. Their cell walls also have an uneven thickness increasing toward the center.

The central cylinder that occupies on average a significantly larger area of the total root section than that in the control sample consists of a pericycle and conducting tissues (Table 1). Moreover, the absolute total area of conducting tissues in all experimental samples is significantly less than in the control. Pericycle cells are arranged in one layer, slightly elongated along the radius and have thin shells. Behind the pericycle, there are the cells that form the conducting tissues. The vascular bundles in the contaminated samples, as well as in the control, are built according to the radial type, but the radial symmetry is not well-defined. Xylem cells are arranged in groups in the form of rays (2–4 pieces) that radiate from the periphery to the center.

Morphometric analysis has shown that the average cortical cell size of contaminated samples is on average less than that in the control samples, while the number of cells per unit area is approximately the same (Table 1).

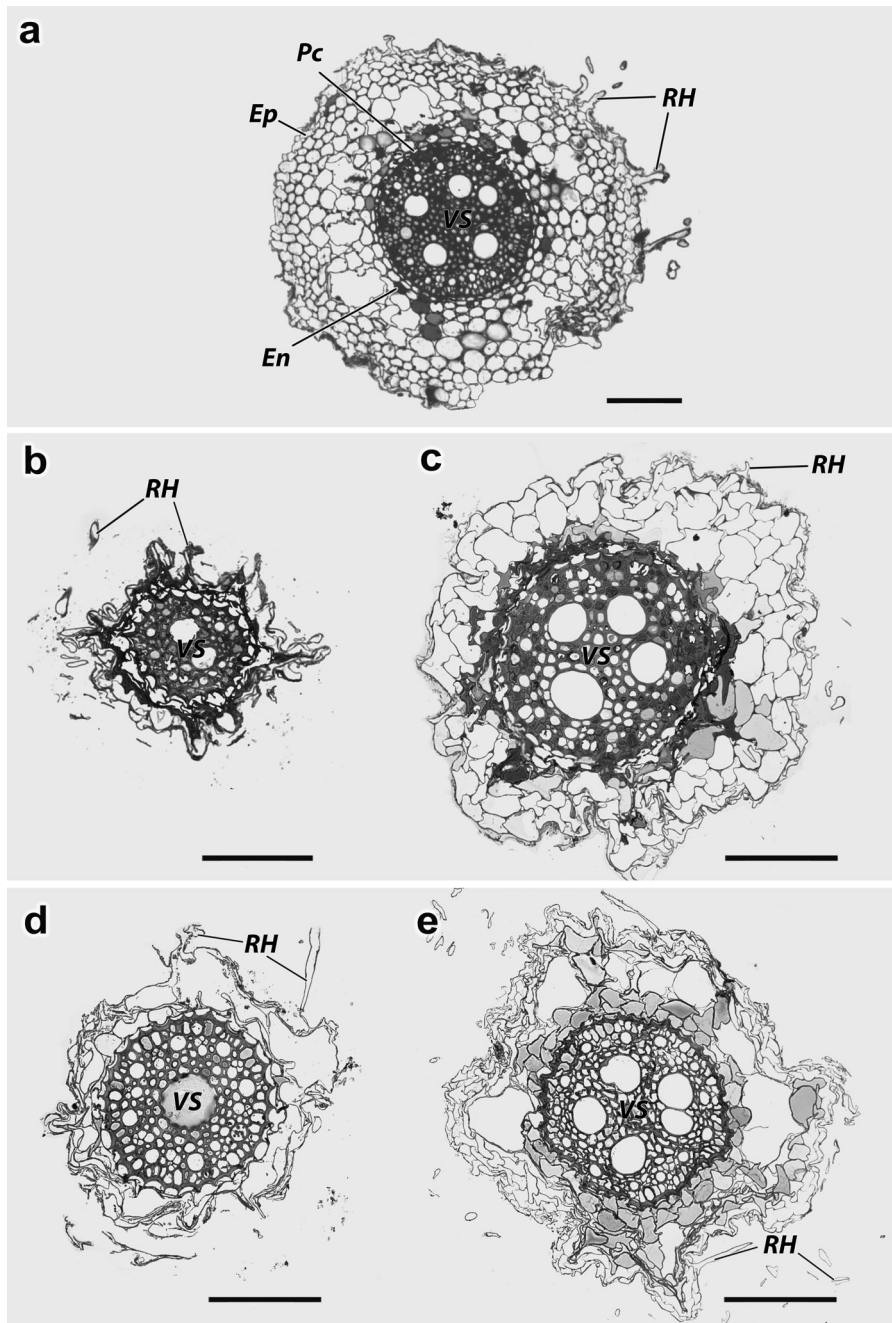


Fig. 1 Cross section of barley root under various levels of soil contamination with copper oxides: **a** control, **b** 300 mg/kg CuO, **c** 2000 mg/kg CuO, **d** 300 mg/kg nano-CuO, **e** 2000 mg/kg

nano-CuO. *RH* root hairs, *Ep* epidermis, *En* endoderm, *Pc* pericycle, *CC* central cylinder

Nano-CuO contamination

The anatomical root structure of the barley samples grown in the soil contaminated with nano-copper

oxide has several significant differences compared to the structure of roots in both the control samples and those grown under CuO contamination. Similarly, to CuO-contaminated samples, the outermost epidermal

Table 1 Cytomorphometric characteristics of the root tissue cells of barley grown in soil with various levels of CuO and nano-CuO contamination

Experiment variants	Average number of cells per 1 mm ²	Average cell size (μm ²)	The total cross-sectional area of the conducting tissues (μm ²)	The ratio of the conducting tissue area to the total root cut area
Control	3773 ± 43	430 ± 37	31,560 ± 294	0.17
CuO 300 mg/kg	4171 ± 58	169 ± 19	20,070 ± 135	0.42
CuO 2000 mg/kg	3246 ± 42	147 ± 12	30,714 ± 201	0.31
nano-CuO 300 mg/kg	3882 ± 49	175 ± 18	22,868 ± 123	0.45
nano-CuO 2000 mg/kg	3143 ± 43	152 ± 23	39,275 ± 328	0.28

layer has live cells with occasional root hairs (Fig. 1d, e). Root hairs are much shorter and less dense than in control.

The cortical cells below the epidermis layer are severely reduced compared to the control samples but are more developed than in the samples contaminated with copper oxide. At a dose of 300 mg/kg of copper nano-oxide, the core layer is approximately the same, while at 2000 mg/kg, it is more developed. The cells of this layer are, on average, larger than in the samples contaminated with copper oxide at the same levels (Table 1). The variants with copper nano-oxide contamination demonstrate large intercellular spaces of the aerenchyma in the core layer (Fig. 1e).

Leaf

Control

Analysis of leaf tissue cells of barley plants grown under zero contamination has shown that mesophyll does not demonstrate a distinct division into columnar and spongy parenchyma. Plants are characterized by an orderly organization and uniform localization of cells in the leaf chlorenchyma (Fig. 3a). Parenchyma cells are located in 4–5 rows between the epidermal layers. They are rounded, rarely highly elongated, elliptical in shape. Parenchyma cells adhere closely to each other forming compact groups with the number of cells up to 8–10 units. The free space between separate compact groups is the intercellular space. Along the sagittal plane of the leaf plate, groups of cells forming conducting bundles are observed. The stomata are located on both sides of the leaf plate.

Morphometric analysis has revealed that the average area of the parenchyma cell is 260 μm², the average number of cells per 1 mm² is 1693 units, the average thickness of the leaf plate is 194 μm and the

ratio of the parenchyma area to the section area of the leaf is 0.65 (Table 2).

Electron microscopic analysis of control leaf samples has shown that the parenchyma cells generally have the ultrastructure typical of higher plants (Fig. 4a). The cells contain an average of 9.8 chloroplasts (Table 2) that are oval in shape and surrounded by a double membrane. Their matrix has an insignificant electron density, against which membrane structures are clearly visible. Inside the chloroplasts, there is a well-developed membrane system represented by stroma thylakoids and grana thylakoids. Grana are well extended; the number of thylakoids is 15–30 units. Plastoglobules and starch grains are rare. Mitochondria are ellipsoidal or bean-shaped and look moderately swollen and, in general, adhere closely to plastids. Their matrix has a slightly lower electron density than plastids and contains a certain number of flattened and drop-shaped cristae. The nucleus is round in shape, and nuclear chromatin is evenly distributed throughout the nucleoplasm. The cytoplasm is located along the cell wall and adheres closely to it. The central part of the cell is occupied by a large vacuole.

CuO and nano-CuO contamination

The structure of the mesophyll cells of the samples grown under both types of contamination (copper oxide and nano-oxide) is generally similar to the structure and localization of the cells of the control samples, while there are certain quantitative differences (Fig. 3b, c). The parenchyma does not demonstrate a distinct division into columnar and spongy. The cells in this layer are round, arranged in several rows and grouped around the vascular bundles. The intercellular space of this tissue is better defined compared to that of the control samples. A quantitative

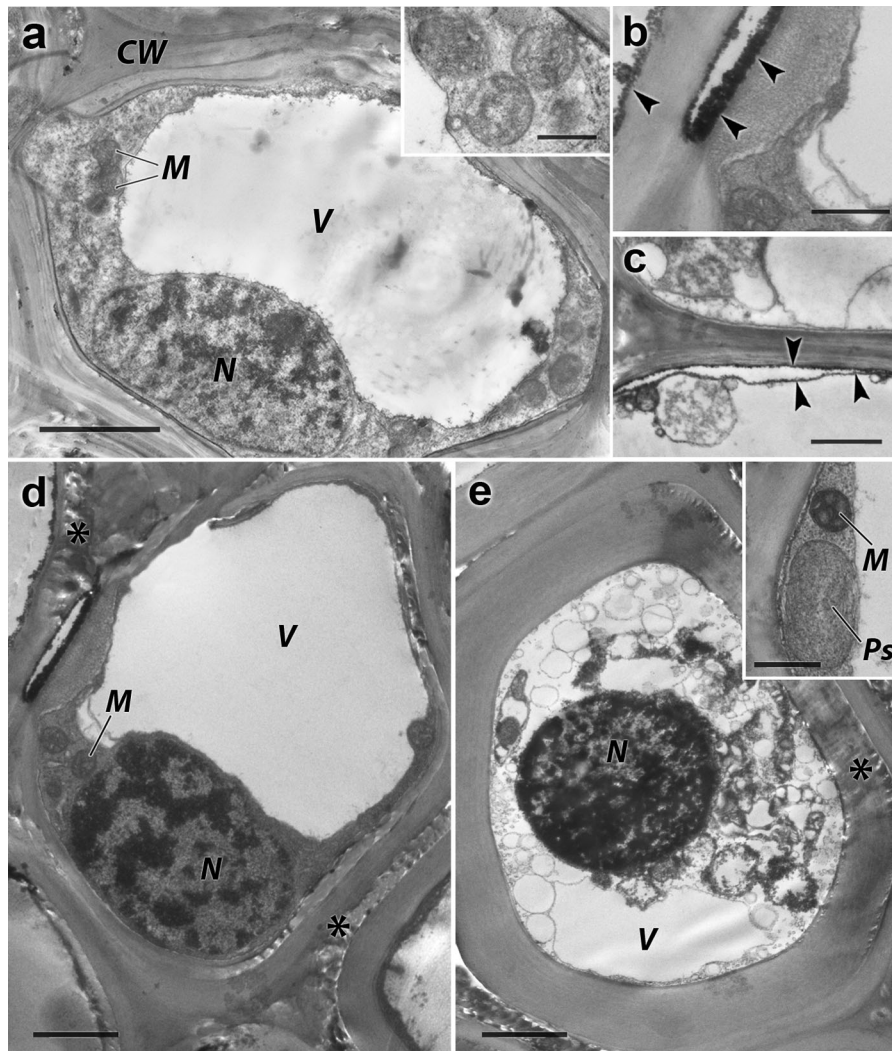


Fig. 2 Central cylinder cell of a barley root: **a** control, **d** nano-CuO contamination, **e** CuO contamination. CW cell wall, V vacuole, M mitochondria, N nucleus, Pr proplastid, N nucleus.

A fragment of a barley root cell under contamination with **b** nano-CuO and **c** CuO. Arrows—electron-dense substance

assessment has showed significant differences in the average size of parenchyma cells (the higher the contamination, the smaller the cells), in the number of cells per unit area (the number of cells per unit area increases with the increase in pollution levels) (Table 2).

The average thickness of the leaf plate and the ratio of the parenchyma area to the total area of the leaf also correspond to the level of contamination: The higher the pollution, the “worse” the indicators. At the same levels of contamination with copper oxide and nano-oxide, the average cell size, the number of cells per unit area and the ratio of parenchyma area to section

area of a leaf are larger for samples grown under copper nano-oxide contamination, while the thickness of a leaf plate is greater for samples with copper oxide contamination (Table 2).

Electron microscopic study has shown that the parenchyma cells of a barley leaf grown under contamination with copper oxides and nano-oxides are round in shape, the cytoplasm is located along the cell wall and a large vacuole—in the center (Fig. 4c). The vacuole content in the samples contaminated with copper oxide in a macrodispersed form either appears transparent or has an electron-light dispersed content uniformly scattered throughout the vacuole. In the

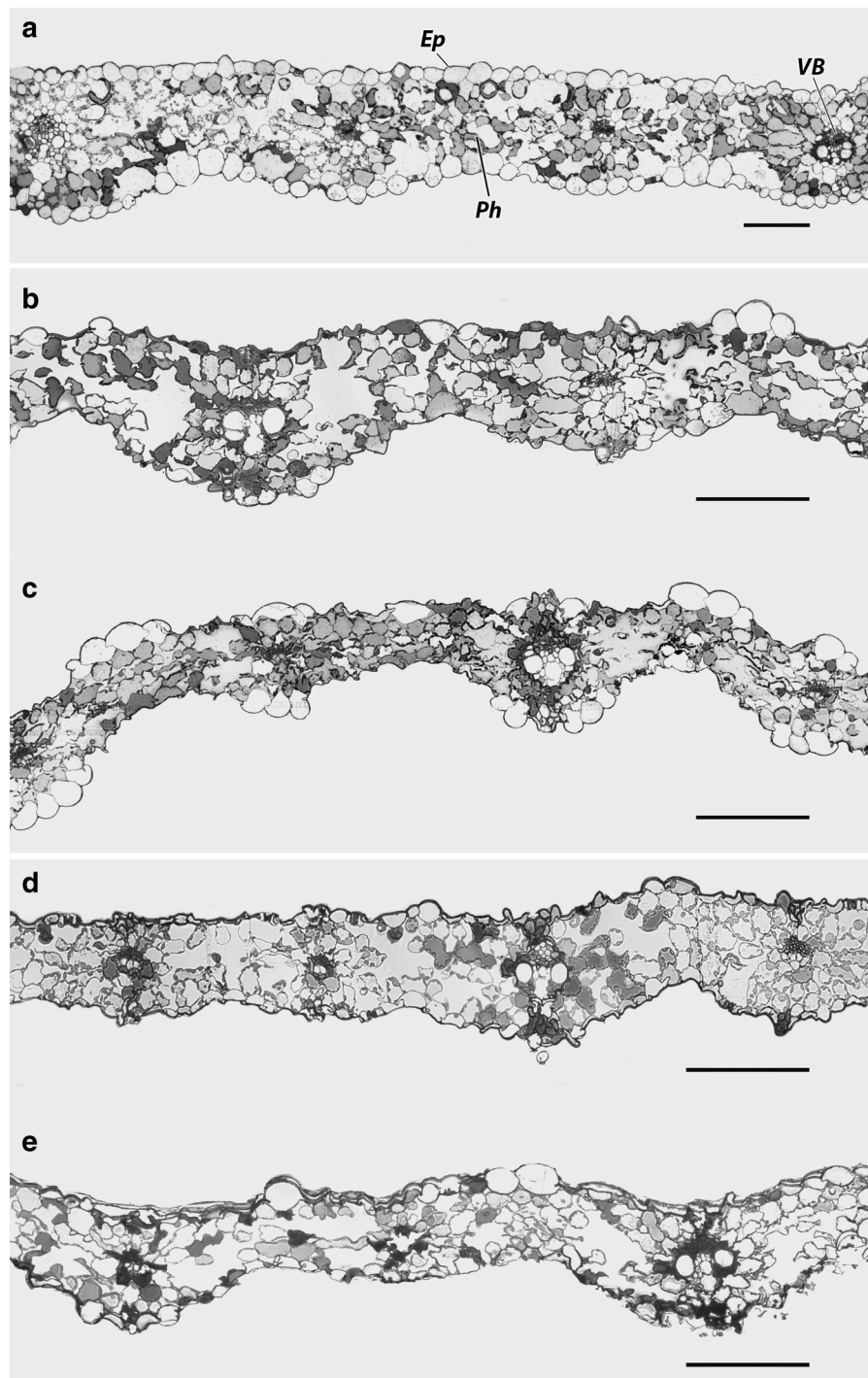


Fig. 3 Cross section of barley leaf: **a** control; **b** 300 mg/kg CuO, **c** 2000 mg/kg CuO, **d** 300 mg/kg nano-CuO, **e** 2000 mg/kg nano-CuO. *Ep* epidermis, *CB* conducting bundles

samples contaminated with copper nano-oxide, parenchyma cell vacuoles contain electron-dense

inclusions grouped in the center of the vacuole which are probably deposits of copper nano-oxide compounds.

Table 2 Cytomorphometric characteristics of parenchyma cells of barley leaf grown in soils with various levels of Cu oxides and nano-oxides contamination

Experiment variants	Average number of cells per 1 mm ²	Average cell size (μm ²)	The leaf plate thickness (μm)	The ratio of the parenchyma area to the leaf section area	The number of plastids per cell
Control	1693 ± 26	260 ± 23	194 ± 9	0.65	9.8 ± 0.87
CuO 300 mg/kg	2302 ± 38	175 ± 19	102 ± 8	0.43	7.7 ± 0.63
CuO 2000 mg/kg	2432 ± 31	146 ± 16	94 ± 7	0.43	6.1 ± 0.56
nano-CuO 300 mg/kg	2750 ± 41	234 ± 27	94 ± 7	0.60	6.5 ± 0.64
nano-CuO 2000 mg/kg	3078 ± 39	168 ± 21	87 ± 8	0.56	5.7 ± 0.54

The number of plastids per leaf parenchyma cell under all types of contamination is less than in the control sample (Table 2). Chloroplasts in the variants contaminated with both copper oxide and nano-dispersed metal forms are elongated, oval and surrounded by a double membrane. Their matrix has an insignificant electron density, against which membrane structures are clearly visible. The membrane system represented by stroma thylakoids and grana thylakoids is adequately developed but is still worse than the one in the control.

Thylakoid grana stacks are shorter in length, in number and in total occupy a smaller volume in the chloroplast. In the variant with copper oxide contamination, grana thylakoids and stroma thylakoids are oriented along the long axis of the chloroplast (Fig. 4d), whereas in the variant contaminated with copper nano-oxide, the membrane system looks more chaotic; in individual chloroplasts, the grana stacks are oriented in different directions (Fig. 4d, e inserts). Starch grains are small and extremely rare. The number and size of plastoglobules are approximately the same in both variants of the experiment and significantly larger than in the control samples. Mitochondria in the variant under copper oxide contamination look condensed and contain a dense matrix and numerous moderately swollen cristae (Fig. 4d insert). Spiral-like membrane formations—lysed material—are found near mitochondria in the cytoplasm. This indicates pathological processes in the cell. In the variant under nano-oxide contamination, mitochondria are larger, the matrix is enlightened, cristae are flattened and evenly distributed throughout the stroma (Fig. 4e) and lysed material is not found.

Discussion

TEM has proved that copper contamination in the form of oxide and nano-oxide has caused ultrastructural changes in the main cellular organelles in the root, which in turn has led to changes in the tissue level. This is one of the reasons for the violation of radial transport and the movement of mineral nutrients from the roots to the stem (Perevolotskaya and Anisimov 2018). It should be noted that the degree of root trichome degradation has also depended on the level of pollution; the stronger the pollution, the less developed the trichomes. Some previously conducted studies showed that excess copper could also cause damage to cell membranes as a result of copper binding to sulfhydryl groups in membrane proteins (Rico et al. 2011; Rajput et al. 2018b). It was indicated that Cu accumulation occurred either through the apoplastic pathway, or it could be associated with carbohydrate fractions, pectin and cell wall proteins. Thus, the plant root cell wall was found to be the site of highest Cu localization.

The present TEM studies have confirmed the presence of electron-dense material on the cell walls and in the plasmolemma of barley root cells under both types of contamination. TEM–EDX methods have allowed detecting the presence of copper in the elemental composition of the electron-dense material (Fig. 5). Within the areas containing the electron-dense precipitate, measurements have shown K and L series spectral lines corresponding to Cu atoms. The measurements obtained in this study are consistent with the results of other authors who carried out studies on heavy metal absorption in hydroponic rice using X-ray diffraction analysis and identified electron-dense material in the root structures as Cu deposits (Peng et al. 2015).

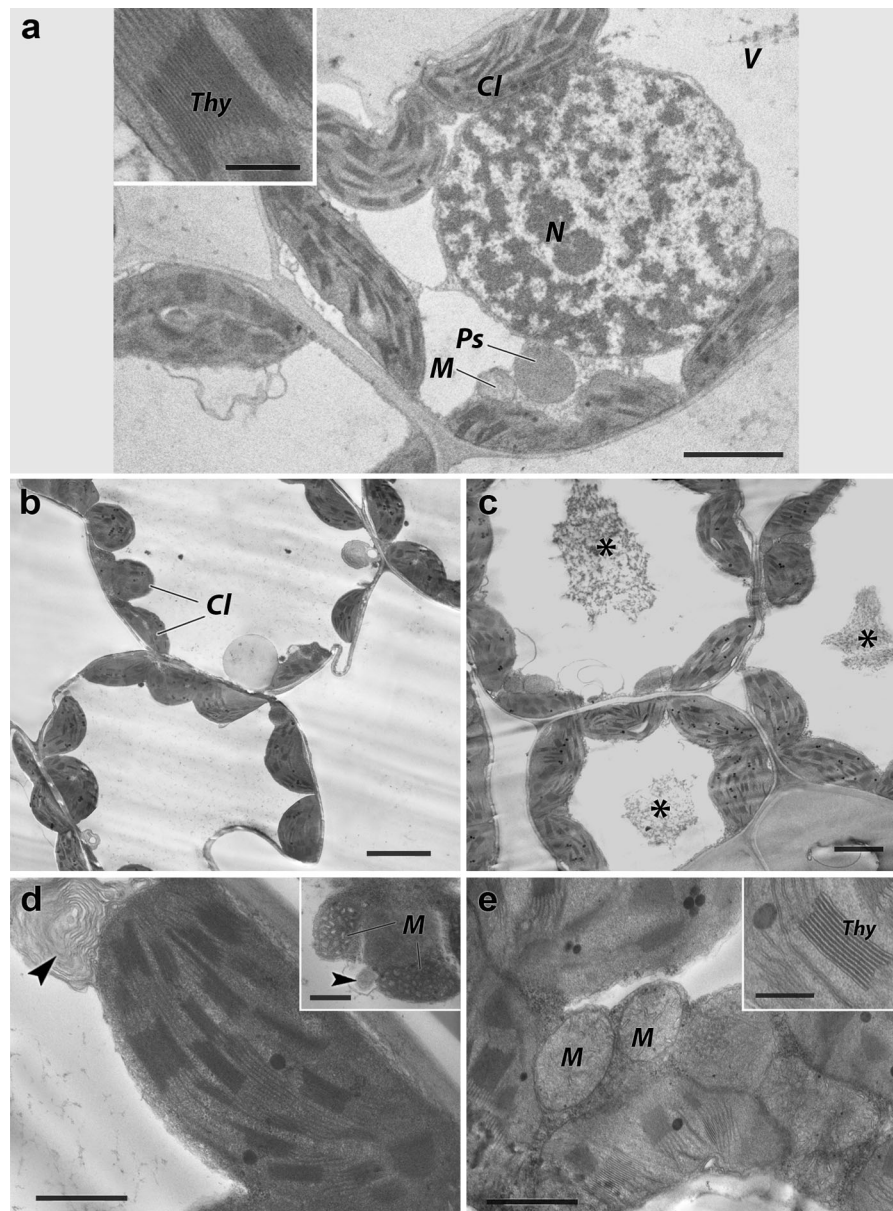


Fig. 4 Barley leaf parenchyma cell: **a** control; **b, d** CuO contamination; **c, e** nano-CuO contamination. *Chl* chloroplast, *V* vacuole, *M* mitochondria, *N* nucleus, *CW* cell wall, *Pr*

peroxisome, *TG* thylakoid grana, *TS* thylakoid stroma, * spiral membrane formations, arrow electron-dense inclusions

Ultrastructural studies of barley leaves have revealed changes in the main cellular organelles under the contamination of barley with copper oxide and nano-oxide. In general, the cellular ultrastructure of the test samples indicates a decrease in metabolic processes. Being compared on the degree of contamination, all variants have demonstrated approximately the same intensity of nonspecific changes in

ultrastructure. The system of intercellular cells in the samples contaminated with oxides is more developed than in the samples with nano-oxide contamination. This allows for more intensive processes of water and gas exchange. The number and size of chloroplasts in the cells have decreased compared to the control with both variants of contamination. Both variants with copper contamination have also demonstrated the

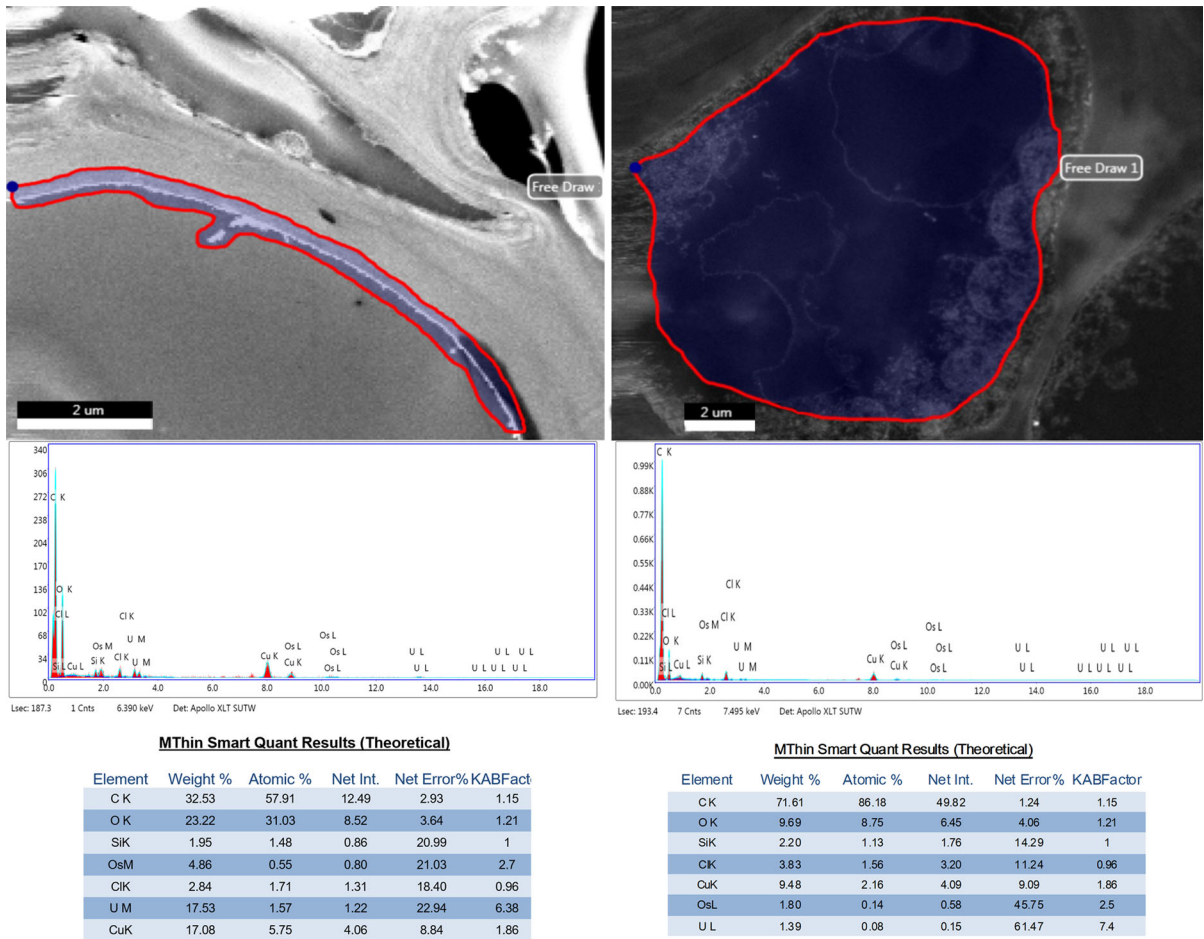


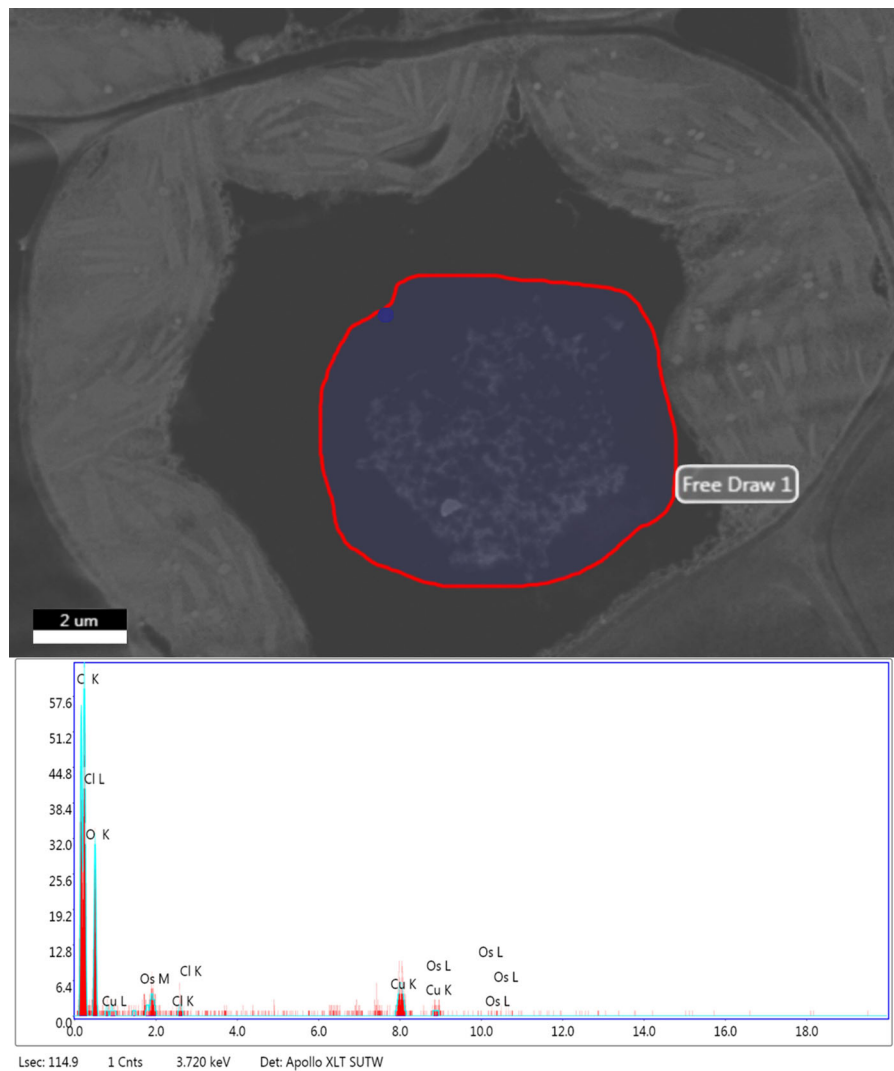
Fig. 5 Electron microscopic image of barley root cells grown under contamination with: **a** CuO, **b** nano-CuO (STEM mode). Spectrogram of the selected area. Table of chemical elements detected

disorganization of the membrane systems of grana and stroma thylakoids. The state of mitochondria has changed. The destructive changes detected in these organelles are obviously associated with a decrease in the level of metabolic processes responsible for ensuring plant growth. The number of plastoglobules has increased, and the number and size of starch grains in plastids have decreased (copper oxides- and nano-oxide-contaminated variants); spiral-shaped membrane formations (variant contaminated with copper oxide) and electron-dense material in central vacuoles (variant contaminated with copper nano-oxide) have been observed. X-ray spectral analysis has shown the presence of copper atoms in them (Fig. 6).

The presence of copper is likely to be associated with the direct entry of both copper oxide nanoparticles and copper ions into the cell on dissolving metal

nanoparticles. The dissolution of nanoparticles depends both on their nature and on such indicators as particle size, surface area and the properties of the medium. Large amounts of Cu^{2+} can be released from copper oxide nanoparticles both in suspension and in the cell medium (Gunawan et al. 2011). Copper oxide nanoparticles and Cu^{2+} ions located in the extracellular space can pass through the cell membrane and enter the cytoplasm through endocytosis and through copper transport proteins (or copper transporter proteins), respectively (Hou et al. 2017).

Copper localization on cell walls and vacuoles can be the main reason for the high copper detoxification in plants (Rajput et al. 2018b; Minkina et al. 2019). The study suggested 70–90% Cu was accumulated in cell wall of perennial herb (*Athyrium yokoscense*) (Nishizono et al. 1987). Similarly, accumulation of Cu



MThin Smart Quant Results (Theoretical)

Element	Weight %	Atomic %	Net Int.	Net Error%	KABFactor
C K	25.89	45.02	2.92	8.16	0.94
O K	31.80	41.51	3.37	6.37	1
ClK	3.71	2.19	0.46	29.52	0.86
CuK	32.20	10.58	1.87	13.34	1.83
OsL	6.39	0.70	0.31	54.85	2.17

Fig. 6 Electron microscopic image of barley leaf cells grown under contamination with copper nano-oxide (STEM mode). Spectrogram of the selected area. Table of chemical elements detected

in the parenchyma cells was observed in the vacuoles and cell walls in studies conducted on *Eichhornia crassipes* (Vesk et al. 1999) and *Avicennia marina* (MacFarlane and Burchett 2000). Accumulation of Cu

occurred either through the apoplastic pathway or it could be associated with the carbohydrate fractions, pectin and cell wall proteins (Krzyszowska et al. 2010). The deposition of xenobiotics penetrated into the cell

in vacuoles, which is a relatively safe and remote place from cytoplasmic processes, can significantly reduce their toxic effect (Kvesitadze et al. 2005). The changes we have noted in chloroplasts, mitochondria and peroxisomes were also found by other researchers to occur in the leaves of *Origanum vulgare*, along with severe damage to organelles and the disappearance of starch grains (Ouzounidou et al. 1992; Panou-Filotheou et al. 2001). They considered the toxicity of Cu to reduce the number and volume of chloroplasts, the content of chlorophyll and, therefore, to reduce the intensity of the photosynthesis process. The plants treated with Cu solutions demonstrated an increase in the number of plastoglobules (Zhang et al. 2010). The structures located in chloroplasts were active centers that synthesize and process proteins under stress. Plastoglobules create a functional metabolic link between the inner and thylakoid membranes and play a key role in the mechanism of protection against oxidative stress (Ytterberg et al. 2006).

Conclusion

The influence of heavy metals, contamination with copper oxide in macro- and nano-dispersed forms studied as an example, has had a negative influence on the development of spring barley. A greater toxic effect has been exerted by the introduction of CuO nanoparticles as compared to the macrodispersed form. A comparative analysis of the toxic effects of copper oxides and nano-oxides on plants has shown changes in the tissue and intracellular levels in the roots of barley. However, qualitative changes in plant leaves under the influence of copper in macro- and nano-dispersed forms have not practically been observed.

Taking into account cytomorphometric, ultrastructural data and data on the copper content in plants, in general, conclusions can be made that copper oxide in nano-dispersed form penetrates better from the soil into the plant and can accumulate in large quantities in it.

One of the main mechanisms of copper oxide nanoparticle toxicity is assumed to be oxidative stress caused by the dissolution of copper oxide nanoparticles entering the cell. Further, more research is required to identify reasons for the detected

differences in sorption behavior between nanoparticulate copper and copper ions.

Acknowledgements This research was supported by the Russian Scientific Foundation, No. 19-74-10046. Analytical work was carried out on the equipment of Centers for collective use of Southern Federal University “Modern microscopy” and “High Technology.”

References

- Anjum, N. A., Gill, S. S., Duarte, A. C., et al. (2013). Silver nanoparticles in soil–plant systems. *Journal of Nanoparticle Research*, 15, 1–26. <https://doi.org/10.1007/s11051-013-1896-7>.
- Arendt, E. K., & Zannini, E. (2013). *Cereal grains for the food and beverage industries* (p. 512). Amsterdam: Woodhead Publishing Limited.
- Assadian, E., Zarei, M. H., Gilani, A. G., et al. (2017). Toxicity of copper oxide (CuO) nanoparticles on human blood lymphocytes. *Biological Trace Element Research*, 184(2), 350–357. <https://doi.org/10.1007/s12011-019-01678-7>.
- Bauer, T., Pinski, D., Minkina, T., Nevidomskaya, D., Mandzhieva, S., Burachevskaya, M., et al. (2018). Time effect on the stabilization of technogenic copper compounds in solid phases of Haplic Chernozem. *Science of the Total Environment*, 626, 1100–1107.
- Conway, J. R., Hanna, S. K., Lenihan, H. S., & Keller, A. A. (2014). Effects and implications of trophic transfer and accumulation of CeO₂ nanoparticles in a marine mussel. *Environmental Science and Technology*, 48, 1517–1524. <https://doi.org/10.1021/es404549u>.
- Costa, D. M. V. J., & Sharma, P. K. (2016). Effect of copper oxide nanoparticles on growth, morphology, photosynthesis, and antioxidant response in *Oryza sativa*. *Photosynthetica*, 54, 110. <https://doi.org/10.1007/s11099-015-0167-5>.
- Darlington, T. K., Neigh, A. M., Spencer, M. T., Nguyen, O. T., & Oldenburg, S. J. (2009). Nanoparticle characteristics affecting environmental fate and transport through soil. *Environmental Toxicology and Chemistry*, 28(6), 1191–1199.
- Dmitrakov, L. M., & Dmitrakova, L. K. (2006). Lead translocation in oat plants. *Agrochemistry*, 2, 71–77. (in Russian).
- Du, W., Tan, W., Yin, Y., Ji, R., Peralta-Videa, J. R., Guo, H., et al. (2018). Differential effects of copper nanoparticles/microparticles in agronomic and physiological parameters of oregano (*Origanum vulgare*). *Science of the Total Environment*, 618, 306–312.
- Fedorenko, G. M., Fedorenko, A. G., Minkina, T. M., et al. (2018). Method for hydrophytic plant sample preparation for light and electron microscopy (studies on *Phragmites australis* Cav.). *MethodsX*, 5, 1213–1220. <https://doi.org/10.1016/j.mex.2018.09.009>.
- Festa, R. A., & Thiele, D. J. (2011). Copper: an essential metal in biology. *Current Biology*, 21, 877–883. <https://doi.org/10.1016/j.cub.2011.09.040>.

- Gabbay, J., Borkow, G., Mishal, J., Magen, E., Zatcoff, R., & Shemer-Avni, Y. (2006). Copper oxide impregnated textiles with potent biocidal activities. *Journal of Industrial Textiles*, 35, 323–335. <https://doi.org/10.1177/1528083706060785>.
- Gomes, T., Pinheiro, J. P., Cancio, I., et al. (2011). Effects of copper nanoparticles exposure in the mussel *Mytilus galloprovincialis*. *Environmental Science and Technology*, 45, 9356–9362. <https://doi.org/10.1021/es200955s>.
- Griffitt, R. J., Hyndman, K., Denslow, N. D., & Barber, D. S. (2009). Comparison of molecular and histological changes in zebrafish gills exposed to metallic nanoparticles. *Toxicological Sciences*, 107(2), 404–415. <https://doi.org/10.1093/toxsci/kfn256>.
- Gunawan, C., Teoh, W. Y., Marquis, C. P., & Amal, R. (2011). Cytotoxic origin of copper (II) oxide nanoparticles: comparative studies with micron-sized particles, leachate, and metal salts. *ACS Nano*, 5, 7214–7225. <https://doi.org/10.1021/nm2020248>.
- Guzman, K. A., Finnegan, M. P., & Banfield, J. F. (2006). Influence of surface potential on aggregation and transport of titania nanoparticles. *Environmental Science and Technology*, 40(24), 7688–7693.
- Hänsch, R., & Mendel, R. R. (2009). Physiological functions of mineral micronutrients (Cu, Zn, Mn, Fe, Ni, Mo, B, Cl). *Current Opinion in Plant Biology*, 12(3), 259–266. <https://doi.org/10.1016/j.pbi.2009.05.006>.
- Hartwig, A. (2013). Metal interaction with redox regulation: an integrating concept in metal carcinogenesis? *Free Radical Biology and Medicine*, 55, 63–72. <https://doi.org/10.1016/j.freeradbiomed.2012.11.009>.
- Hou, J., Wang, X., Hayat, T., & Wang, X. (2017). Ecotoxicological effects and mechanism of CuO nanoparticles to individual organisms. *Environmental Pollution*, 221, 209–217.
- Hu, W., Culloty, S., Darmody, G., et al. (2014). Toxicity of copper oxide nanoparticles in the blue mussel, *Mytilus edulis*: A redox proteomic investigation. *Chemosphere*, 108, 289–299. <https://doi.org/10.1016/j.chemosphere.2014.01.054>.
- Ivask, A., Bondarenko, O., Jepihina, N., & Kahru, A. (2010). Profiling of the reactive oxygen species related eco-toxicity of CuO, ZnO, TiO₂, silver and fullerene nanoparticles using a set of recombinant luminescent *Escherichia coli* strains: differentiating the impact of particles and solubilised metals. *Analytical and Bioanalytical Chemistry*, 398, 701–716. <https://doi.org/10.1007/s00216-010-3962-7>.
- Julich, D., & Gäth, S. (2014). Sorption behavior of copper nanoparticles in soils compared to copper ions. *Geoderma*, 235–236, 127–132. <https://doi.org/10.1016/j.geoderma.2014.07.003>.
- Kahru, A., & Ivask, A. (2013). Mapping the dawn of nanoecotoxicological research. *Accounts of Chemical Research*, 46(3), 823–833. <https://doi.org/10.1021/ar3000212>.
- Keller, A., McFerran, S., Lazareva, A., et al. (2013). Global life cycle releases of engineered nanomaterials. *Journal of Nanoparticle Research*, 15, 1692. <https://doi.org/10.1007/s11051-013-1692-4>.
- Krzyszowska, M., Lenartowska, M., Samardakiewicz, S., Bilski, H., & Woźny, A. (2010). Lead deposited in the cell wall of *Funaria hygrometrica* protonemata is not stable—a remobilization can occur. *Current Opinion in Plant Biology*, 15(8), 325–338.
- Kulizhsky, S., Loyko, S., & Lim, A. (2013). Pedotransfer capacity of nickel and platinum nanoparticles in Albeluvisols Haplic in the South-East of the Western Siberia. *Eurasian J. Soil Sci.*, 2(2), 90–96.
- Kvesitadze, G. I., Khatishashvili, G. A., Sadunishvili, T. A., & Evstigenyeva, Z. G. (2005). *Metabolism of anthropogenic toxicants in higher plants* (p. 199). Moscow: Publishing House Science. (in Russian).
- Lecoanet, H. F., Bottero, J.-Y., & Wiesner, M. R. (2004). Laboratory assessment of the mobility of nanomaterials in porous media. *Environmental Science and Technology*, 38(19), 5164–5169.
- Ma, X., Geiser-Lee, J., Deng, Y., & Kolmakov, A. (2010). Interactions between engineered nanoparticles (ENPs) and plants: phytotoxicity, uptake and accumulation. *Science of the Total Environment*, 408(16), 3053–3061. <https://doi.org/10.1016/j.scitotenv.2010.03.031>.
- MacFarlane, G. R., & Burchett, M. D. (2000). Cellular distribution of copper, lead and zinc in the grey mangrove, *Avicennia marina* (Forsk.) Vierh. *Aquatic Botany*, 68, 45–59.
- McVay, I. R., Maher, W. A., Krikowa, F., & Ubrhien, R. (2019). Metal concentrations in waters, sediments and biota of the far south-east coast of New South Wales, Australia, with an emphasis on Sn, Cu and Zn used as marine antifoulant agents. *Environmental Geochemistry and Health*, 41, 1351–1367.
- Minkina, T. M., Fedorov, Y. A., Nevidomskaya, D. G., Pol'shina, T. N., Mandzhieva, S. S., & Chaplygin, V. A. (2017). Heavy metals in soils and plants of the don river estuary and the Taganrog Bay coast. *Eurasian Soil Science*, 50(9), 1033–1047. <https://doi.org/10.1134/S1064229317070067>.
- Minkina, T., Rajput, V., Fedorenko, G., Fedorenko, A., Mandzhieva, S., Sushkova, S., et al. (2019). Anatomical and ultrastructural responses of *Hordeum sativum* to the soil spiked by copper. *Environmental Geochemistry and Health*. <https://doi.org/10.1007/s10653-019-00269-8>.
- Morgalev, Yu N, Khoch, N. S., Morgaleva, T. G., et al. (2010). Biological testing of nanomaterials: on the possibility of nanoparticles translocation into food networks. *Russian Nanotechnologies*, 5, 131–135. <https://doi.org/10.1134/S1995078010110157>.
- Musante, C., & White, J. C. (2012). Toxicity of silver and copper to Cucurbita pepo: Differential effects of nano and bulk-size particles. *Environmental Toxicology*, 27, 510–517.
- Navratilova, J., Praetorius, A., Gondikas, A., Fabienke, W., von der Kammer, F., & Hofmann, T. (2015). Detection of engineered copper nanoparticles in soil using single particle ICP-MS. *International Journal of Environmental Research and Public Health*, 12(12), 15756–15768. <https://doi.org/10.3390/ijerph121215020>.
- Nishizono, H., Ichikawa, H., Suzuki, S., & Ishii, F. (1987). The role of the root cell wall in the heavy metal tolerance of *Athyrium yokoscense*. *Plant and Soil*, 101, 15–20.
- Oberdörster, G., Stone, V., & Donaldson, K. (2007). Toxicology of nanoparticles: A historical perspective. *Nanotoxicology*, 1, 2–25. <https://doi.org/10.1080/17435390701314761>.

- Ouzounidou, G., Eleftheriou, E., & Karataglis, S. (1992). Eco-physiological and ultrastructural effects of copper in *Thlaspi ochroleucum* (Cruciferae). *Canadian Journal of Botany*, *70*, 947–957.
- Panou-Filotheou, H., Bosabalidis, A. M., & Karataglis, S. (2001). Effects of copper toxicity on leaves of oregano (*Origanum vulgare* subsp. *hirtum*). *Annals of Botany*, *88*, 207–214. <https://doi.org/10.1006/anbo.2001.1441>.
- Peng, C., Duan, D. C., Xu, C., et al. (2015). Translocation and biotransformation of CuO nanoparticles in rice (*Oryza sativa* L.) plants. *Environmental Pollution*, *197*, 99–107. <https://doi.org/10.1016/j.envpol.2014.12.008>.
- Perevolotskaya, T. V., & Anisimov, V. S. (2018). Conceptual and mathematical statement of the process of heavy metals migration in the system soil–agricultural plant. *Bio-geosystem Technique*, *5*(1), 110–128. <https://doi.org/10.13187/bgt.2018.1.110>.
- Phenrat, T., Kim, H.-J., Fagerlund, F., Illangasekare, T., Tilton, R. D., & Lowry, G. V. (2009). Particle size distribution, concentration, and magnetic attraction affect transport of polymer-modified Fe⁰ nanoparticles in sand columns. *Environmental Science and Technology*, *43*(13), 5079–5085.
- Rajput, V., Minkina, T., Ahmed, B., Sushkova, S., Singh, R., Soldatov, M., et al. (2020). Interaction of copper-based nanoparticles to soil, terrestrial, and aquatic systems: Critical review of the state of the science and future perspectives. *Reviews of Environmental Contamination and Toxicology*, *252*, 51–96. https://doi.org/10.1007/398_2019_34.
- Rajput, V., Minkina, T., Sushkova, S., Behal, A., Maksimov, A., Blicharska, E., et al. (2019). ZnO and CuO nanoparticles: A threat to soil organisms, plants, and human health. *Environmental Geochemistry and Health*. <https://doi.org/10.1007/s10653-019-00317-3>.
- Rajput, V., Minkina, T. M., Fedorenko, A. G., et al. (2018a). Toxicity of copper oxide nanoparticles on spring barley (*Hordeum sativum* distichum). *Science of the Total Environment*, *645*, 1103–1113. <https://doi.org/10.1016/j.scitotenv.2018.07.211>.
- Rajput, V. D., Minkina, T., Suskova, S., et al. (2018b). Effects of copper nanoparticles (CuO NPs) on crop plants: A mini review. *BioNanoSci*, *8*, 36–42. <https://doi.org/10.1007/s12668-017-0466-3>.
- Rico, C. M., Majumdar, S., Duarte-Gardea, M., Peralta-Videa, J. R., & Gardea-Torresdey, J. L. (2011). Interaction of nanoparticles with edible plants and their possible implications in the food chain. *Journal of Agriculture and Food Chemistry*, *59*, 3485–3498. <https://doi.org/10.1021/jf104517j>.
- Shaw, A. K., & Hossain, Z. (2013). Impact of nano-CuO stress on rice (*Oryza sativa* L.) seedlings. *Chemosphere*, *93*, 906–915. <https://doi.org/10.1016/j.chemosphere.2013.05.044>.
- Tutayuk, V. H. (1972). *Anatomy and morphology of plants. Textbook for agricultural universities* (p. 336). Moscow: Higher School Publishing House. (in Russian).
- Usatov, A. V., Fedorenko, G. M., Shcherbakova, L. B., & Mashkina, E. V. (2004). Ultrastructure of chloroplasts in mustard *Brassica juncea* as an index of salt tolerance. *Tsitologiya*, *46*, 1035–1042.
- Vesk, P. A., Nockolds, C. E., & Allaway, W. G. (1999). Metal localization in water hyacinth roots from an urban wetland. *Plant, Cell and Environment*, *22*, 149–158.
- Xiong, T., Dumat, C., Dappe, V., Vezin, H., Schreck, E., Shahid, M., et al. (2017). Copper oxide nanoparticle foliar uptake, phytotoxicity, and consequences for sustainable urban agriculture. *Environmental Science and Technology*, *51*, 5242–5251.
- Ytterberg, A. J., Peltier, J. B., & van Wijk, K. J. (2006). Protein profiling of plastoglobules in chloroplasts and chromoplasts. A surprising site for differential accumulation of metabolic enzymes. *Plant Physiology*, *140*, 984–997.
- Zhang, N., He, X. D., Gao, Y. B., Li, Y. H., Wang, H. T., Ma, D., et al. (2010). Pedogenic carbonate and soil dehydrogenase activity in response to soil organic matter in *Artemisia ordosica* community. *Pedosphere*, *20*, 229–235. [https://doi.org/10.1016/s1002-0160\(10\)60010-0](https://doi.org/10.1016/s1002-0160(10)60010-0).
- Zuverza-Mena, N., Medina-Velo, I. A., Barrios, A. C., Tan, W., Peralta-Videa, J. R., & Gardea-Torresdey, J. L. (2015). Copper nanoparticles/compounds impact agronomic and physiological parameters in cilantro (*Coriandrum sativum*). *Environmental Science: Processes & Impacts*, *17*, 1783–1793. <https://doi.org/10.1039/c5em00329f>.

Publisher's Note Springer Nature remains neutral with regard to jurisdictional claims in published maps and institutional affiliations.